

Interaction effects with varying N in $SU(N)$ symmetric fermion lattice systems

Shenglong Xu,^{1,2} Julio T. Barreiro,¹ Yu Wang,³ and Congjun Wu¹

¹*Department of Physics, University of California, San Diego, California 92093, USA*

²*Condensed Matter Theory Center and Department of Physics,
University of Maryland, College Park, Maryland 20742, USA*

³*School of Physics and Technology, Wuhan University, Wuhan 430072, China*

The interaction effects in ultracold Fermi gases with $SU(N)$ symmetry are studied non-perturbatively in half-filled one-dimensional lattices by employing quantum Monte Carlo simulations. We find that as N increases, weak and strong interacting systems are driven to a crossover region, but from opposite directions as a convergence of itinerancy and Mottness. In the weak interaction region, particles are nearly itinerant, and inter-particle collisions are enhanced by N , resulting in the amplification of interaction effects. In contrast, in the strong coupling region, increasing N softens the Mott-insulating background through the enhanced virtual hopping processes. The crossover region exhibits nearly N -independent physical quantities, including the relative bandwidth, Fermi distribution, and the spin structure factor. The difference between even- N and odd- N systems is most prominent at small N 's with strong interactions, since the odd case allows local real hopping with an energy scale much larger than the virtual one. The above effects can be experimentally tested in ultracold atom experiments with alkaline-earth (-like) fermions such as ^{87}Sr (^{173}Yb).

PACS numbers:

High symmetry groups (e.g. $SU(N)$, $Sp(N)$, and $SO(N)$) are typically investigated in the context of high-energy physics. They were introduced to condensed matter physics as a tool to apply the $1/N$ -expansion to handle strong correlation effects in realistic $SU(2)$ electronic systems [1–4]. High symmetries enhance quantum spin fluctuations and suppress antiferromagnetic Néel ordering [1, 2, 5, 6], which has stimulated intensive efforts to study exotic quantum paramagnetic states, such as valence-bond solid states and spin liquid states with high symmetries [7–13]. However, high symmetries are rare in solids in spite of many multi-component spin systems. For example, in transition-metal-oxides, Hund's coupling aligns electron spins forming large spin moments. However, the symmetry remains $SU(2)$, and quantum spin fluctuations are suppressed by the large spin.

Ultracold atom systems open up new possibilities to study high symmetries since many alkali and alkaline-earth fermions carry hyperfine spins larger than $\frac{1}{2}$. It was first pointed out that spin- $\frac{3}{2}$ fermionic systems exhibit a generic $Sp(4)$ symmetry without fine tuning [14–16], which is further enlarged to $SU(4)$ for spin-independent interactions, a feature of alkaline-earth fermions. Magnetic and superfluid properties of large spin fermion systems, many of which possess high symmetries, have been systematically studied [17–24]. The past few years have witnessed a significant experimental progress along this direction. High symmetries, such as $SU(6)$ and $SU(10)$, are realized with ^{173}Yb [25] and ^{87}Sr atoms [26, 27], respectively. The interplay between the nuclear-spin and electronic-orbital degrees of freedom leads to complex physics [8, 28, 29]. Moreover, various $SU(N)$ symmetric quantum degenerate gases and Mott insulators in optical lattices have been realized [25–28, 30–37].

A natural question on $SU(N)$ symmetric fermion systems is how fermion correlations vary with N . When the total fermion density is fixed, the Bethe-ansatz solution for one-dimensional (1D) systems shows that the low energy properties approach those of spinless bosons as $N \rightarrow \infty$ [20, 38]. As N becomes large, more and more fermions can antisymmetrize their spin wavefunctions such that their orbital wavefunctions are more symmetrized in mimicking bosons. In a more interesting scenario, the density is fixed, but N varies, as realized in a recent experiment [37]: By using a subset of the spin-projection components of ^{173}Yb atoms, 1D $SU(N)$ systems were constructed with up to $N = 6$. Increasing N intensifies inter-particle collisions, and thus the Fermi distribution is broadened as N increases. This experiment was performed in the metallic region where the interaction effect is weak.

It would be interesting to explore further the consequences of a high symmetry in the lattice, in particular, when the system is in Mott-insulating states, for example, at half-filling. In this letter, we systematically investigate the half-filled 1D $SU(N)$ lattice systems, i.e., $N/2$ particles per site on average, by using quantum Monte-Carlo (QMC) simulations. These systems are insulating in the ground states of both weak and strong interaction regions, but the interaction effects scale differently as N increases when expressed in terms of the relative bandwidth W_R (the ratio of the kinetic energies in the interacting and free systems), Fermi distribution, and spin structure factor. In the weak interaction region, the interaction effects are strengthened as N increases. In contrast, in the strong interaction region, increasing N softens the Mott-insulating background and weakens correlations. There exists a crossover region characterized

by nearly N -independent relative bandwidths and spin structure factors. To our knowledge, such a crossover phenomenon as the symmetry grows has not been investigated before. Previous large- N studies in the condensed matter literature typically focus on Heisenberg models by freezing the charge fluctuations, which are already in the infinite- U limit. Our work is different from previous studies by directly working on Hubbard models that include both charge and spin physics. Due to the local charge fluctuations of odd- N systems, they exhibit an opposite N -dependence of the relative bandwidths and stronger dimerization compared to the even- N case at small values of N . As N increases, such difference is diminished by strong charge fluctuations.

We consider the 1D $SU(N)$ Hubbard model,

$$H = -t \sum_{\langle ij \rangle, \alpha} c_{i, \alpha}^\dagger c_{j, \alpha} + \frac{U}{2} \sum_i n_i (n_i - 1) - \mu \sum_i n_i, \quad (1)$$

where $\langle \rangle$ represents the nearest-neighboring bond; the spin index α runs from 1 to N ; $n_i = \sum_\alpha c_{i, \alpha}^\dagger c_{i, \alpha}$ is the total particle number at site i . This model possesses a particle-hole symmetry at half-filling, which fixes $\mu = \frac{N-1}{2}U$.

We will investigate quantitatively the correlation effects that arise as N varies from 2 to larger values, by employing QMC, a method well-known to be free of the sign problem in the path-integral framework in 1D at any filling. The stochastic-series-expansion (SSE) QMC method will be applied with the directed-loop algorithm [39], which allows us to perform large-scale simulations efficiently. We will focus on insulating states at half-filling and a system size set to $L = 100$ for all simulations below. The finite size effects were verified to be negligible for all the quantities reported here.

The ground states of the half-filled $SU(N)$ Hubbard chains described by Eq. 1 are insulating at $U > 0$ with charge gaps opening for all values of $N \geq 2$ [18, 40–42]. Except for the $SU(2)$ case in which the spin sector remains gapless exhibiting algebraic antiferromagnetic (AFM) ordering, spin gaps open for $N \geq 3$ accompanied by the appearance of dimerization. In the weak interaction region, there is no qualitative difference between the even and odd N cases. Increasing N enhances fermion collisions among different components, which strengthens both charge and spin gaps. However, in the strong interaction region $U \gg t$, the physics is qualitatively different between even and odd N 's. For illustration, consider a two-site problem filled with N fermions, which is discussed in detail in the Supplementary Material (SM.) I [43]. When N is even, each site holds $\frac{N}{2}$ fermions on average. Weak charge fluctuations arise from virtual hoppings, generating the AFM super-exchange $J \approx 4t^2/U$. In contrast, when N is odd, the onsite charge fluctuations remain significant even at the limit $U \rightarrow \infty$ due to the real hopping of one particle in the background of $\frac{N-1}{2}$ particles on each site. In both cases, the ground state

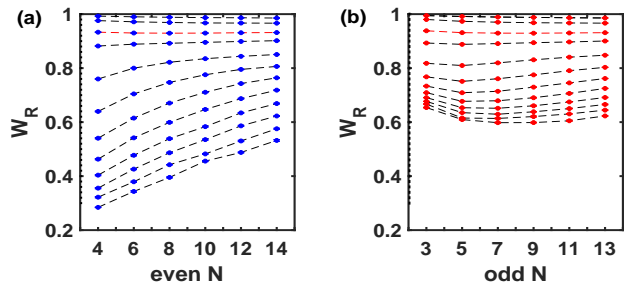


FIG. 1: The relative bandwidth W_R for even (a) and odd (b) N at $\beta = 30$. In both cases, the dashed lines shown as a guide from top to bottom correspond to $U/t = 0.5, 1.0, 2.0, 3.0, 5.0, 7.0, 9.0, 11.0, 13.0, 15.0, 17.0, 19.0$, respectively. The cross-over lines with $U/t \approx 2$ (marked red) separating the weak and strong interaction regions are nearly N -independent. (a) For even N , W_R decreases with N in the weak interaction region, while it increases in the strong interaction region. (b) For odd N , the behavior for weak interactions is similar to (a). However, in the strong interaction regime, W_R is non-monotonic, first decreasing and then increasing with N .

is an $SU(N)$ singlet, and the first excited states belong to the $SU(N)$ adjoint representation. The spin gap for even values of N is $\Delta_s \approx \frac{N}{2}J$, while that for odd values of N is $\Delta_s \approx t$. The single-particle gap for adding one particle/hole is estimated as $\Delta_{spg} \approx U$ when N is even and $\Delta_{spg} \approx \frac{N+1}{2}t$ when N is odd. Since dimerization develops in the 1D lattice for $N \geq 3$, the picture based on two sites already captures the essential physics in the thermodynamic limit. As N increases to U/t , the system crosses over into the weak interaction region, and the distinction between even and odd N cases smears.

To support the above physical intuitions, we perform QMC simulations at a very low temperature to approach the ground states. ($\beta = t/T = 30$ is used for Figs. 1, 2, and 3.) The bandwidth narrowing is a characteristic feature of Mott insulators, which often shows in spectroscopy measurements in solids. We define the relative bandwidth $W_R = E_K/E_K^0$ where E_K is the kinetic energy at the interaction U , and E_K^0 is the corresponding non-interacting value. $W_R = 1$ in the non-interacting case, and it is completely suppressed to zero at $U = \infty$. At finite values of U , the N -dependence of W_R from the weak to strong interaction regions is plotted in Fig. 1 (a) for even N and (b) for odd N . These curves do not cross since W_R monotonically decreases as U increases. For small values of U/t , the single-particle gap Δ_{spg} is exponentially small, and thus fermions remain nearly itinerant over a long correlation length $\xi \propto t/\Delta_{spg}$, with the lattice constant set as 1. Increasing N strengthens the inter-particle collisions, and W_R decreases monotonically for both even and odd N .

Conversely, in the strong coupling region, a distinct even-odd effect appears. For N even, W_R is significantly

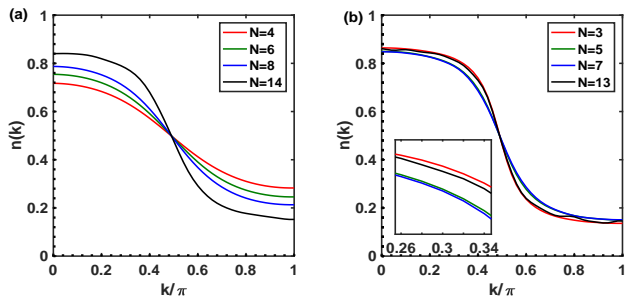


FIG. 2: Momentum distribution $n(k)$ in the strong interaction region for even (a) and odd (b) values of N . Parameter values are $U/t = 15$ and $\beta = 30$. All curves cross at $n(k_f = \frac{\pi}{2}) = \frac{1}{2}$. (a) For even N 's, $n(k)$ is driven towards the weak interaction distribution limit as N increases. (b) For odd N 's, $n(k)$ exhibits non-monotonic behavior as N increases, which is consistent with that of the W_R shown in Fig. 1 (b).

below 1 due to the suppression of charge fluctuations. The virtual hopping processes dominate, whose number per bond scales as $(\frac{N}{2})^2$, thus W_R increases roughly linearly with N . For odd values of N , the overall scale of W_R is larger than that of even N 's, since both the real and virtual hopping processes contribute to W_R . When N is small, the real hopping dominates, since its kinetic energy scale is on the order of t , which is much larger than J of the virtual hopping. Similar to the weak interaction case, W_R goes down initially as N increases, which enhances inter-particle collisions. As N grows, the virtual hopping takes over, since the number per bond scales as $(\frac{N-1}{2})^2$, while that of the real hopping scales as $\frac{N+1}{2}$. Consequently, after passing a minima, W_R increases with N . The value of N at the turning point can be determined by equating the energy scale of the real hopping $\frac{N+1}{2}t$ to the virtual one $(\frac{N-1}{2})^2J$ with $J = 4t^2/U$, yielding $N \approx U/2t$. After that, the system crosses over from the strong to the intermediate interaction region. Then W_R behaves similarly for both even and odd N .

Between the weak and strong interaction regions, there exist a crossover area. Say, along the line of $U/t \approx 2$, $W_R \approx 0.9$ is nearly N -independent, as shown in both Fig. 1 (a) and (b). For N even, as N increases, W_R approaches the crossover from opposite directions in the weak and strong interaction regions. For N odd, W_R behaves similarly as N becomes large. This observation implies that the limits of $U \rightarrow 0$ and $N \rightarrow \infty$ are non-exchangeable. For the non-interacting limit, $\lim_{N \rightarrow \infty} \lim_{U \rightarrow 0} (1 - W_R) = 0$. Moreover, we conjecture the existence of an interacting large- N limit

$$\lim_{U \rightarrow 0} \lim_{N \rightarrow \infty} (1 - W_R) \approx 0.1. \quad (2)$$

The smearing of the Fermi distribution, which is defined as $n(k) = \frac{1}{N} \sum_{\alpha} \langle c_{\alpha,k}^{\dagger} c_{\alpha,k} \rangle$, is an indication of correlation. It can be measured via time-of-flight spectra in cold atom systems [37]. Below we present the

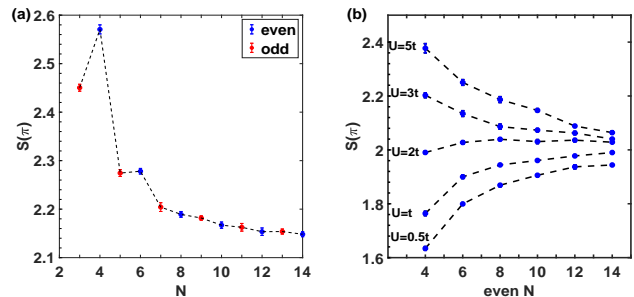


FIG. 3: The N -dependence of $S(Q = \pi)$ at $\beta = 30$. (a) At $U/t = 15$ (strong interaction), $S(\pi)$ for $N = 2m - 1$ and $2m$ are close, and the latter is slightly larger. As N increases, $S(\pi)$ drops rapidly showing the suppression of AFM correlations. (b) Similar to W_R , $S(\pi)$ exhibits opposite N -dependence in the weak and strong interaction regions. The crossover occurs around $U/t \approx 2$, consistent with W_R shown in Fig. 1 (a).

QMC results of the N -dependence of $n(k)$ in the strong interaction region at a very low temperature for even and odd N 's in Fig. 2 (a) and (b), respectively. At $U = +\infty$, $n(k)$ is completely flattened. Nevertheless, at finite values of U , short-range charge fluctuations render $n(k_i) > n(k_f) > n(k_o)$, where $k_i < k_f < k_o$ and the Fermi wavevector $k_f = \frac{\pi}{2}$. Compared to the ideal Fermi distribution, $n(k)$ is significantly smeared and becomes continuous at k_f . Due to the particle-hole symmetry, $n(k) = 1 - n(\pi - k)$ holds for all N 's at half-filling, thus all curves cross at $n(k_f) = \frac{1}{2}$. When N is even, $n(k)$ is less smeared as N increases, which enhances charge fluctuations on the Mott insulating background. In contrast, the experiment done in 1D optical tubes observed a broadening of $n(k)$, which is a feature of the weak-interaction metallic region [37]. In our simulations, a similar behavior appears in the weak interaction region where the fermion itinerancy remains significant. When N is odd, $n(k)$'s dependence on N is much weaker. It also exhibits non-monotonic behavior as N increases, which is consistent with W_R 's.

Quantum magnetic correlation is a fundamental property in the Mott insulating states reflected by the spin structure factor $S(Q)$, which can be measured through the noise correlations of the time-of-flight spectra [44]. $S(Q)$ is the Fourier component at momentum Q of the two-point spin correlation function $C_s(i, j)$ defined as

$$C_s(i, j) = \frac{1}{2C(N)} \sum_{\alpha\beta} \langle S_{\alpha\beta}(r_i) S_{\beta\alpha}(r_j) \rangle, \quad (3)$$

where $S_{\alpha\beta}(r_i) = c_{i,\alpha}^{\dagger} c_{i,\beta} - \frac{n_i}{N} \delta_{\alpha\beta}$; $C(N)$ is defined to normalize $C_s = 1$ for $i = j$ in the limit of large U , as shown in the SM. II [43]. The antiferromagnetic correlation is reflected by $S(Q = \pi)$, which is studied for varying N and U below. In Fig. 3 (a), $S(Q)$ in the strong interaction region ($U/t = 15$) is presented. Again consider a two-site problem in the large- U limit for intuition: The

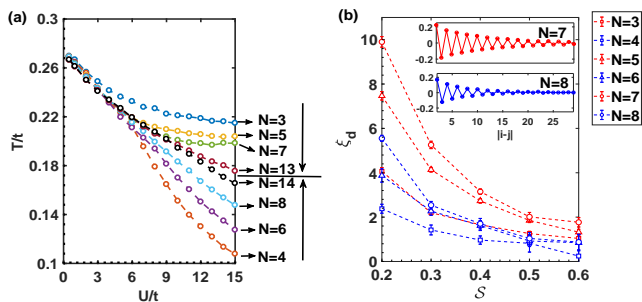


FIG. 4: (a) The T - U relations during the adiabatic process with a fixed specific entropy $\mathcal{S}/k_B = 0.3$. As U increases to the strong interaction region, the isoentropy curves with even and odd N 's behave differently, and they merge together from opposite directions in the large- N limit. (b) The dimer correlation length ξ_d v.s. the specific entropy \mathcal{S} . The correlation length increases with N in general. The odd- N systems (red) overall exhibit stronger dimerization instability than the even- N ones (blue). In the inset, the real space correlation function $C_d(i, j)$ is shown for $N = 7$ and $N = 8$ for comparison at $\mathcal{S}/k_B = 0.2$.

number of resonating spin configurations is $(2m)!/(m!)^2$ for both $N = 2m - 1$ and $2m$. Consequently, $S(Q)$ for $N = 2m - 1$ and $2m$ are close to each other. Nevertheless, the odd- N case has a prominent dimerization tendency facilitated by stronger charge fluctuations, thus $S(Q)$ at $N = 2m$ is larger. Overall, $S(Q)$ decreases rapidly with increasing N , which enhances spin fluctuations. In Fig. 3 (b), the N -dependence of $S(Q)$ is presented for even N by varying U . Similar to W_R , there exists a crossover region, say, $S(Q)$ is nearly independent on N around $U/t \approx 2$, which is approached in opposite directions from weak and strong interaction regions. The N -dependence at odd N 's is similar as presented in SM. II [43].

Finite entropy- Now we consider the finite temperature (entropy) properties. In cold-atom lattice experiments, the entropy per particle \mathcal{S} , or specific entropy, is a more convenient parameter than temperature T . The $\mathcal{S}(T)$ relation can be obtained via

$$\mathcal{S}(T) = \ln 4 + \frac{E(T)}{T} - \int_T^\infty dT' \frac{E(T')}{T'^2}, \quad (4)$$

where $\ln 4$ is the entropy at the infinite- T limit and $E(T)$ is the internal energy per particle. We present the isoentropy curves in the T - U plane as adiabatically turning U to the strong interaction region for different N 's in Fig. 4 (a), considering \mathcal{S} below, but close to the experimental availability, say, $\mathcal{S} = 0.3$ [35]. An overall trend is that T decreases as U increases for all N 's as a reminiscence of the Pomeranchuk effect: Increasing U drives the system more local-moment like, and thus T decreases to maintain \mathcal{S} invariant [45–48]. The temperatures as U becomes large for even N 's are lower than those of odd N 's because fermions in the even N case are more local-moment-like and possess higher entropy capacity than the odd N case.

When N is even, as shown in previous studies [46, 47], increasing N softens the Mott gap and drives the system less local-moment-like, which reduces the entropy capacity, and thus T increases as N increases. In contrast, there are still significant local charge fluctuations in the odd N case even in the large U region. Increasing N further enhances the collision among fermions, and reduces the fermion itinerary, which increases the entropy capacity and reduces the temperature. This is in sharp contrast to the case of $1/N$ -filling investigated before, in which T monotonically decreases simply because of the $\ln N$ scaling of the specific entropy [45, 49, 50].

The above even-odd effects can be observed experimentally by measuring the dimerization order. When N is odd, the dimerization ordering is based on the combined effect of real and virtual hoppings: The real hopping dominates if N is small, and the virtual one becomes important as N goes large. Hence, the corresponding dimerization ordering is stronger than that of the even N case which is only based on the virtual hopping. Therefore, we propose that systems with odd N are better candidates to observe the dimerization order compared to those with even N . In particular, systems with odd values of N , $3 \leq N \leq 9$, are experimentally accessible by using ^{173}Yb and ^{87}Sr atoms [25–27]. We define its two-bond correlation function as

$$C_d(i-j) = \frac{1}{N} (\langle K_i K_j \rangle - \langle K_i \rangle \langle K_j \rangle), \quad (5)$$

where $K_i = \sum_\alpha c_{\alpha,i}^\dagger c_{\alpha,i+1} + h.c.$ is the bonding strength between site i and $i+1$. The dimer correlation length ξ_d is simulated by fitting $C_d(i-j) \propto e^{-|i-j|/\xi_d}$. Its dependence on \mathcal{S} and N is plotted in Fig. 4 (b) in the strong interaction region. As \mathcal{S} decreases, ξ_d grows much faster in the odd N case. For comparison, $C_d(i-j)$'s are plotted in real space for $N = 7$ and 8 in the inset.

The lowest specific entropy \mathcal{S} reachable in the optical lattice is about at $\sim 0.6k_B$, and in the center of the harmonic trap, it can be lowered to $\sim 0.3k_B$ [35, 51]. We expect that with further improvements in cooling and spectroscopic techniques [32, 33, 52, 53], the dimer ordering could be observed in future $SU(N)$ cold atom experiments. In particular, the following detection protocol would yield the two-bond correlation function above, but for alternating pairs of sites, and revealing its decay. After the realization of the 1D $SU(N)$ Hubbard model with ^{87}Sr for any N in a blue magic-wavelength lattice at 389.9 nm [54], chosen for example and technical convenience, we follow the detection scheme in Refs. [54, 55], but with a bichromatic lattice including one at 2×389.9 nm. However, before band-mapping, when nearest-neighbor singlets-triplets lead to two-band occupation, we selectively [32] and sequentially transfer each band occupation and spin component to a state with a cycling fluorescing transition [56], 3P_2 , which is each then imaged with a quantum gas microscope [57, 58],

ultimately revealing the dimer correlation length.

In conclusion, we have non-perturbatively studied one-dimensional $SU(N)$ fermion lattice systems at half-filling. In the strong interaction region, the odd- N systems exhibit stronger charge fluctuations and dimerization than the even N . As N reaches the level of U/t , the virtual hopping processes dominate in both even and odd N systems, and the interaction effects are weakened for increasing N . Whereas from the weak interaction limit, increasing N enhances particle collisions and strengthens the interaction effect. These two distinct behaviors approach a crossover region around $U \sim 2t$ from opposite directions, as demonstrated in experimentally measurable quantities including the kinetic energy scale, the momentum distribution functions, and spin structure factors. The above pictures of convergence of physics of itineracy and Mottness are not limited to one dimension. It applies to Mott states in two and three dimensions as well. In previous simulations of 2D $SU(2N)$ Hubbard models [48, 59] the softening of the single particle gap for increasing N has been found in at relatively large values of U . A detailed study will be deferred to a future letter.

Acknowledgments S. X. and C. W. are supported by AFOSR FA9550-14-1-0168. Y.W. gratefully acknowledges financial support from the National Natural Science Foundation of China under Grants No. 11729402, No. 11574238, and No. 11328403. Y.W. is also grateful for the award of a scholarship funded by the China Scholarship Council (File No. 201706275082). C. W. and J. B. acknowledge support from the President's Research Catalyst Awards of the University of California.

-
- [1] I. Affleck and J. B. Marston, Phys. Rev. B **37**, 3774 (1988).
- [2] D. P. Arovas and A. Auerbach, Phys. Rev. B **38**, 316 (1988).
- [3] N. Read and S. Sachdev, Phys. Rev. Lett. **66**, 1773 (1991).
- [4] S. Sachdev and N. Read, Int. J. Mod. Phys. B **05**, 219 (1991).
- [5] J. B. Marston and I. Affleck, Phys. Rev. B **39**, 11538 (1989).
- [6] N. Read and S. Sachdev, Phys. Rev. B **42**, 4568 (1990).
- [7] A. Paramekanti and J. B. Marston, J. Phys. Condens. Matter **19**, 125215 (2007).
- [8] M. Hermele, V. Gurarie, and A. M. Rey, Phys. Rev. Lett. **103**, 135301 (2009).
- [9] C. Honerkamp and W. Hofstetter, Phys. Rev. Lett. **92**, 170403 (2004).
- [10] K. Harada, N. Kawashima, and M. Troyer, Phys. Rev. Lett. **90**, 117203 (2003).
- [11] P. Corboz, A. M. Läuchli, K. Penc, M. Troyer, and F. Mila, Phys. Rev. Lett. **107**, 215301 (2011).
- [12] P. Corboz, M. Lajkó, A. M. Läuchli, K. Penc, and F. Mila, Phys. Rev. X **2**, 041013 (2012).
- [13] T. C. Lang, Z. Y. Meng, A. Muramatsu, S. Wessel, and F. F. Assaad, Phys. Rev. Lett. **111**, 066401 (2013).
- [14] C. Wu, J.-P. Hu, and S.-C. Zhang, Phys. Rev. Lett. **91**, 186402 (2003).
- [15] C. Wu, Mod. Phys. Lett. B **20**, 1707 (2006).
- [16] C. Wu, Phys. Rev. Lett. **95**, 266404 (2005).
- [17] M. D. Hoffman, A. C. Loheac, W. J. Porter, and J. E. Drut, Phys. Rev. A **95**, 033602 (2017).
- [18] S. Capponi, P. Lecheminant, and K. Totsuka, Ann. Phys. (N. Y.) **367**, 50 (2016).
- [19] P. He, Y. Jiang, X. Guan, and J. He, Journal of Physics A Mathematical General **48**, 015002 (2015).
- [20] X.-W. Guan, Z.-Q. Ma, and B. Wilson, Phys. Rev. A **85**, 033633 (2012).
- [21] D. Wang, Y. Li, Z. Cai, Z. Zhou, Y. Wang, and C. Wu, Phys. Rev. Lett. **112**, 156403 (2014).
- [22] Z. Zhou, D. Wang, Z. Y. Meng, Y. Wang, and C. Wu, Phys. Rev. B **93**, 245157 (2016).
- [23] T.-L. Ho and B. Huang, Phys. Rev. A **91**, 043601 (2015).
- [24] T.-L. Ho and S. Yip, Phys. Rev. Lett. **82**, 247 (1999).
- [25] H. Hara, Y. Takasu, Y. Yamaoka, J. M. Doyle, and Y. Takahashi, Phys. Rev. Lett. **106**, 205304 (2011).
- [26] B. J. Desalvo, M. Yan, P. G. Mickelson, Y. N. Martinez De Escobar, and T. C. Killian, Phys. Rev. Lett. **105**, 030402 (2010).
- [27] S. Stellmer, R. Grimm, and F. Schreck, Phys. Rev. A **87**, 013611 (2013).
- [28] A. V. Gorshkov, M. Hermele, V. Gurarie, C. Xu, P. S. Julienne, J. Ye, P. Zoller, E. Demler, M. D. Lukin, and A. M. Rey, Nat. Phys. **6**, 289 (2010).
- [29] G. Chen, K. R. A. Hazzard, A. M. Rey, and M. Hermele, Phys. Rev. A **93**, 061601 (2016).
- [30] S. Taie, Y. Takasu, S. Sugawa, R. Yamazaki, T. Tsujimoto, R. Murakami, and Y. Takahashi, Phys. Rev. Lett. **105**, 190401 (2010).
- [31] F. Scazza, C. Hofrichter, M. Höfer, P. C. De Groot, I. Bloch, and S. Fölling, Nat. Phys. **10**, 779 (2014).
- [32] X. Zhang, M. Bishof, S. L. Bromley, C. V. Kraus, M. S. Safronova, P. Zoller, A. M. Rey, and J. Ye, Science **345**, 1467 (2014).
- [33] S. Taie, R. Yamazaki, S. Sugawa, and Y. Takahashi, Nat. Phys. **8**, 825 (2012).
- [34] P. M. Duarte, R. A. Hart, T.-L. Yang, X. Liu, T. Paiva, E. Khatami, R. T. Scalettar, N. Trivedi, and R. G. Hulet, Phys. Rev. Lett. **114**, 070403 (2015).
- [35] A. Omran, M. Boll, T. A. Hilker, K. Kleinlein, G. Salomon, I. Bloch, and C. Gross, Phys. Rev. Lett. **115**, 263001 (2015).
- [36] C. Hofrichter, L. Riegger, F. Scazza, M. Höfer, D. R. Fernandes, I. Bloch, and S. Fölling, Phys. Rev. X **6**, 021030 (2016).
- [37] G. Pagano *et al.*, Nat. Phys. **10**, 198 (2014).
- [38] C. N. Yang and Y.-Z. You, Chinese Phys. Lett. **28**, 020503 (2011).
- [39] O. F. Syljuåsen and A. W. Sandvik, Phys. Rev. E Stat. Nonlin. Soft Matter Phys. **66**, 046701 (2002).
- [40] R. Assaraf, P. Azaria, E. Boulat, M. Caffarel, and P. Lecheminant, Phys. Rev. Lett. **93**, 016407 (2004).
- [41] P. Azaria, arxiv: 1011.2944 (2010).
- [42] H. Nonne, P. Lecheminant, S. Capponi, G. Roux, and E. Boulat, Phys. Rev. B **84**, 125123 (2011).
- [43] See Supplemental Material for further explanations and additional technical details, which includes Ref. [60].
- [44] E. Altman, E. Demler, and M. D. Lukin, Phys. Rev. A **70**, 13603 (2004).

- [45] K. R. A. Hazzard, V. Gurarie, M. Hermele, and A. M. Rey, Phys. Rev. A **85**, 041604 (2012).
- [46] Z. Cai, H.-h. Hung, L. Wang, D. Zheng, and C. Wu, Phys. Rev. Lett. **110**, 220401 (2013).
- [47] Z. Zhou, Z. Cai, C. Wu, and Y. Wang, Phys. Rev. B **90**, 235139 (2014).
- [48] Z. Zhou, D. Wang, C. Wu, and Y. Wang, Phys. Rev. B **95**, 085128 (2017).
- [49] L. Bonnes, K. R. A. Hazzard, S. R. Manmana, A. M. Rey, and S. Wessel, Phys. Rev. Lett. **109**, 205305 (2012).
- [50] L. Messio and F. Mila, Physical review letters **109**, 205306 (2012).
- [51] T. Paiva, Y. L. Loh, M. Randeria, R. T. Scalettar, and N. Trivedi, Phys. Rev. Lett. **107**, 086401 (2011).
- [52] C. J. M. Mathy, D. A. Huse, and R. G. Hulet, Phys. Rev. A **86**, 023606 (2012).
- [53] R. A. Hart, P. M. Duarte, T.-L. Yang, X. Liu, T. Paiva, E. Khatami, R. T. Scalettar, N. Trivedi, D. A. Huse, and R. G. Hulet, Nature **519**, 211 (2015).
- [54] M. S. Safronova, Z. Zuhrianda, U. I. Safronova, and C. W. Clark, Phys. Rev. A **92**, 040501 (2015).
- [55] D. Greif, T. Uehlinger, G. Jotzu, L. Tarruell, and T. Esslinger, Science **340**, 1307 (2013).
- [56] A. Daley, M. Boyd, J. Ye, and P. Zoller, Phys. Rev. Lett. **101**, 170504 (2008).
- [57] M. Miranda, R. Inoue, Y. Okuyama, A. Nakamoto, and M. Kozuma, Phys. Rev. A **91**, 063414 (2015).
- [58] R. Yamamoto, J. Kobayashi, T. Kuno, K. Kato, and Y. Takahashi, New J. Phys. **18**, 023016 (2016).
- [59] Z. Cai, H.-H. Hung, L. Wang, and C. Wu, Phys. Rev. B **88**, 125108 (2013).
- [60] S. R. Manmana *et al.*, Phys. Rev. A **84**, 043601 (2011).

Supplemental Material: Interaction effects from the parity of N in $SU(N)$ symmetric fermion lattice systems

Shenglong Xu,¹ Julio Barreiro,¹ Yu Wang,² and Congjun Wu¹

¹*Department of Physics, University of California, San Diego, California 92093, USA*

²*School of Physics and Technology, Wuhan University, Wuhan 430072, China*

We present a few details supporting the conclusions in the main text, including estimating the single particle gap Δ_{spg} and the spin gap Δ_s based on the two-site picture for both even and odd N cases, the density-matrix-renormalization-group (DMRG) calculation of the gaps for the $SU(3)$ case, and the discussion on the $SU(N)$ spin correlations.

I. THE TWO-SITE PROBLEM

In this section, we solve the two-site problem in the large- U limit for both even and odd values of N for intuitions. The corresponding single-particle gaps and the spin gaps are calculated.

In the case of even $N = 2m$, each site is filled with m fermions in the large- U limit. The single particle gap is simply $\Delta_{spg} = \frac{U}{2}$. The dimensions of the truncated Hilbert space of this two-site problem is $\left(\frac{(2m)!}{m!m!}\right)^2$. The degeneracy of these states is lifted by considering virtual hopping to high energy states. By performing the 2nd order perturbation theory, the effective Hamiltonian within the truncated Hilbert space is

$$H_{eff}^e = \frac{J}{2} \left(\sum_{\alpha,\beta} S_{\alpha\beta}(1)S_{\beta\alpha}(2) - \frac{N}{4} \right). \quad (1)$$

with $J = \frac{4t^2}{U}$ is the super-exchange energy scale. Its ground state is an $SU(N)$ singlet, denoted as $|G\rangle$, satisfying,

$$(S_{\alpha\beta}(1) + S_{\alpha\beta}(2)) |G\rangle = 0. \quad (2)$$

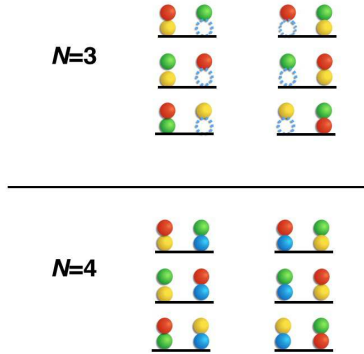


FIG. 1: The resonating spin configurations for a two-site $SU(N)$ singlet in the large- U limit. The numbers of spin configurations are the same for $N = 2m$ and $N = 2m - 1$. Examples of $N = 3$ and $N = 4$ are shown.

Therefore the ground state energy of Eq. (1) is,

$$\begin{aligned} E_g^e(N) &= -\frac{J}{2} \left(\sum_{\alpha,\beta} \langle G | S_{\alpha\beta}(1)S_{\beta\alpha}(1) | G \rangle + \frac{N}{4} \right) \quad (3) \\ &= -\frac{J}{8} N(N+2). \end{aligned}$$

The ground state contains all N fermion components with $\frac{(2m)!}{(m!)^2}$ resonating spin configurations, as shown in Fig. 1. The first excited state belongs to the $SU(N)$ adjoint representation. To obtain the spin gap, one can change one fermion component and calculate the energy difference. Then there are two fermions with the same favor on different sites, which do not contribute to the virtual hopping process. Hence, effectively, the fermion favor numbers are reduced to $N - 2$. Therefore, the lowest energy in this sector is the same as the ground state energy E_g for the case of $N' = N - 2$. In consequence, the spin gap $\Delta_s = E_g^e(N - 2) - E_g^e(N) = \frac{J}{2}N$.

In the case of odd $N = 2m - 1$, each site contains either m or $m - 1$ fermions in the large- U limit at half-filling. The dimensions of the Hilbert space are still $\left(\frac{(2m)!}{m!m!}\right)^2$. Unlike the even- N case, these states are connected through the real hopping. The effective Hamiltonian is

$$H_{eff,o} = -tP \left(\sum_{\alpha} c_{\alpha,1}^{\dagger} c_{\alpha,2} \right) P + h.c., \quad (4)$$

where P is the projection operator into the above physical Hilbert space. The ground state is also an $SU(N)$ singlet. With the filling constraint, one can construct two singlet states $|G\rangle_a$ and $|G\rangle_b$. The former has $m - 1$ and m fermions on site 1 and 2, respectively, and the latter switches the occupation numbers. The ground state is the superposition of these two as

$$|G\rangle = \frac{\sqrt{2}}{2} (|G\rangle_a + |G\rangle_b). \quad (5)$$

The number of the resonating spin configurations is still in total $\frac{(2m)!}{(m!)^2}$ as the same as the case of $N = 2m$ as shown in Fig. 1. To calculate the ground state energy, actually it is easier to compute the expectation value of

H^2 with respect to $\langle H^2 \rangle$, and then take the square root. The expression of $(H_{eff}^0)^2$ is

$$(H_{eff}^0)^2 = -t^2 \left(\sum_{\alpha,\beta} S_{\alpha\beta}(1)S_{\beta\alpha}(2) - \frac{(N+1)^2}{4N} \right). \quad (6)$$

Therefore,

$$\begin{aligned} E_g^o &= -\sqrt{\langle G | (H_{eff}^0)^2 | G \rangle} \\ &= -t \left(\sum_{\alpha,\beta} -\langle G | S_{\alpha\beta}(1)S_{\beta\alpha}(1) | G \rangle + \frac{(N+1)^2}{4N} \right)^{1/2} \\ &= -\frac{N+1}{2}t. \end{aligned} \quad (7)$$

For the second line, we have used Eq. (2) again.

We now discuss the single particle gap and the spin gap of the odd- N systems. After adding an extra fermion to the system, the real hopping processes are completely forbidden by the filling constraint imposed by the strong Hubbard U , and the energy is zero. Therefore, the single particle gap $\Delta_{spg} = \frac{t}{2}(N+1)$. Similar to the even- N case, the spin gap can be obtained by changing one fermion's flavor and calculate the energy difference, then the two fermions with the same flavor occupying different sites do not participate in hopping processes. Hence, the lowest energy in this sector is the ground state energy for $N' = N - 2$, Consequently, the spin gap can be obtained as $\Delta_s = E_g^o(N-2) - E_g^o(N) = t$.

The single-particle and the spin gaps of the two-site problem are summarized as below,

N	even	odd
Δ_{spg}	$\frac{U}{2}$	$\frac{t}{2}(N+1)$
Δ_s	$\frac{J}{2}N$	t

(8)

The above analysis is valid for the strong interaction region $U/t \gg N$, where the even- N systems and odd- N systems exhibit distinct energy scales. We also consider the 2-site problem with a fixed large value of U , say, at $U/t = 10$ by using exact diagonalization. As increasing N , the differences between even and odd values of N diminish. The two kinds of systems approach to the same limit, as shown in Fig. 2, where the N -dependences of both Δ_{spg} and Δ_s are presented.

II. THE DMRG CALCULATIONS FOR THE SU(3) CHAIN

To justify the above argument, we calculate both Δ_{spg} and Δ_s for a 100-site SU(3) Hubbard chain at half-filling, using the DMRG method with bond-dimension 128, and the results are shown in Fig. 3. In the large U limit, both the single-particle gap and the spin gap approach $\sim 0.5t$, drastically different from the even- N case where

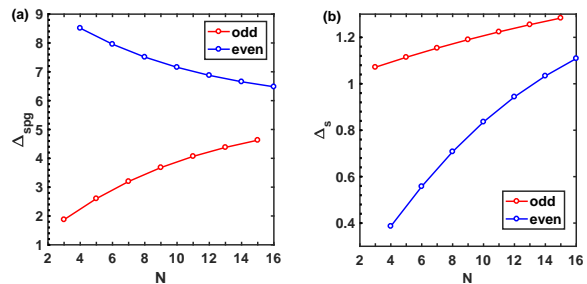


FIG. 2: The N -dependence of the single particle gap Δ_{spg} (a) and the spin gap Δ_s (b) of the two-site problem. The parameter value is $U/t = 20$. As N increases, the different energy scales of Δ_{spg} and Δ_s between even and odd- N cases gradually merge together.

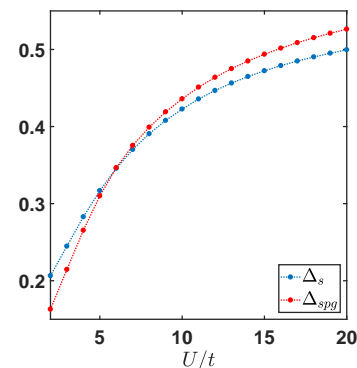


FIG. 3: The U -dependence of the single particle gap Δ_{spg} and the spin gap Δ_s for $N = 3$ based on the DMRG calculations for a lattice with 100 sites and the bond dimension 128. In sharp contrast to the even- N cases, both Δ_{spg} and Δ_s approach finite values at the order of $\sim 0.5t$ as U goes large, consistent with the two-site picture.

$\Delta_{spg} \sim U/2$ and $\Delta_s \sim JN/2$. Compared with two-site picture, the spin gap is reduced to half by the many-body quantum fluctuation.

III. THE SU(N) SPIN CORRELATION FUNCTION

In this section, we provide some details on the spin correlation function defined in the main text,

$$C_s(i, j) = \frac{1}{2C(N)} \sum_{\alpha\beta} \langle S_{\alpha\beta}(r_i) S_{\beta\alpha}(r_j) \rangle, \quad (9)$$

where $S_{\alpha\beta}(r_i) = c_{i,\alpha}^\dagger c_{i,\beta} - \frac{n_i}{N} \delta_{\alpha\beta}$. The normalization factor $C(N)$ is used such that $C_s(i, i) \rightarrow 1$ as $U \rightarrow \infty$. It is straightforward to show that,

$$C_s(i, i) = \frac{1}{2C(N)} \frac{N+1}{N} (N - n_i) n_i, \quad (10)$$

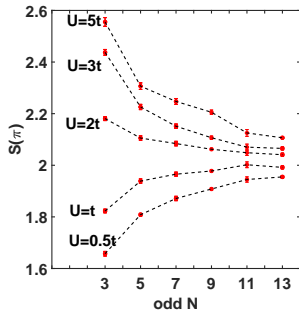


FIG. 4: The N -dependence of the spin structure factor $S(Q = \pi)$ for odd N . It is similar to the case of even N presented in the main text.

where n_i is the on-site particle number operator. In the case of even N , $n_i = N/2$, whereas in the case of odd N , $n_i = (N \pm 1)/2$. Requiring that $C_s(i, i) = 1$, we have

$$C(N) = \begin{cases} \frac{N(N+1)}{8} & \text{if } N \text{ is even;} \\ \frac{(N+1)(N^2-1)}{8N} & \text{if } N \text{ is odd.} \end{cases} \quad (11)$$

In the framework of the SSE Monte Carlo, measuring

the off-diagonal operators involves breaking world-lines and tracking relative positions of the worm-head and tail, and thus is quite complicated. Instead, the diagonal spin correlation function is more convenient to measure¹:

$$\langle C_s^{diag}(i, j) \rangle = \frac{1}{N} \sum_{\alpha} \langle n_i^{\alpha} n_j^{\alpha} \rangle - \frac{1}{N(N-1)} \sum_{\alpha \neq \beta} \langle n_i^{\alpha} n_j^{\beta} \rangle,$$

where $\langle \dots \rangle$ represents the thermal average. In fact, one can show that the $SU(N)$ symmetry implies that

$$\langle C_s(i, j) \rangle = \frac{N^2 - 1}{2C(N)} \langle C_s^{diag}(i, j) \rangle.$$

Therefore, the two kinds of correlation functions are equivalent up to an overall constant.

In Fig 3. (b) of the main text, we have presented the spin structure factor for the case of even N , which shows a crossover behavior between the weak interaction region and the strong interaction region. Here, we present the spin structure factors of odd- N systems in Fig. 4, which show qualitatively the same behavior as the even- N systems.

¹ S. R. Manmana *et al.*, Phys. Rev. A **84**, 043601 (2011).